HHS Public Access

Author manuscript

Prostate. Author manuscript; available in PMC 2020 June 01.

Published in final edited form as:

Prostate. 2019 June ; 79(9): 980–993. doi:10.1002/pros.23809.

Hyperglycemia and T-Cell infiltration are associated with stromal and epithelial prostatic hyperplasia in the Non-obese diabetic (NOD) mouse.

LaTayia M. Aaron-Brooks[1,2], **Takeshi Sasaki**[2,*], **Renee E. Vickman**[2], **Lin Wei**[3], **Omar E. Franco**[2], **Yuan Ji**[3,#], **Susan E. Crawford**[2], and **Simon W. Hayward**[2]

[1]Department of Biochemistry and Cancer Biology, Meharry Medical College, Nashville, TN, USA

[2]Department of Surgery, NorthShore University HealthSystem, Evanston, IL, USA

[3]Program of Computational Genomics & Medicine, NorthShore University HealthSystem, Evanston, IL

Abstract

Background: Prostatic inflammation and various pro-inflammatory systemic co-morbidities, such as diabetes and obesity are associated with human benign prostatic hyperplasia (BPH). There is a paucity of in vivo models reflecting specific aspects of BPH pathogenesis. Our aim was to investigate the non-obese diabetic (NOD) mouse as a potential model for subsequent intervention studies.

Methods: We used the NOD mouse, a model of autoimmune inflammation leading to type 1 diabetes to examine the effects of systemic inflammation and diabetes on the prostate. We assessed changes in prostatic histology, infiltrating leukocytes and gene expression associated with aging and diabetic status.

Results: Both stromal expansion and epithelial hyperplasia were observed concurrently in the prostates. Regardless of diabetic status, the degree of prostatic hyperplasia varied. Local inflammation was associated with a more severe prostatic phenotype in both diabetic and non-diabetic mice. Testicular atrophy was noted in diabetic mice, but prostate glands showed persistent focal cell proliferation. In addition, a prostatic intraepithelial neoplasia (PIN)-like phenotype was seen in several diabetic animals with an associated increase in c-Myc and MMP2 expression. To examine changes in gene and cytokine expression we performed microarray and cytokine array analysis comparing the prostates of diabetic and non-diabetic animals. Microarray analysis revealed several differentially expressed genes including *CCL3*, *CCL12* and *TNFS10*. Cytokine

Corresponding author: Simon W. Hayward Ph.D., Department of Surgery, NorthShore University HealthSystem, Evanston, Illinois, USA, 1001 University Place, Evanston, IL 60201, Tel: 224-364-7672 shayward@northshore.org.

*Current Address: Department of Nephro-Urologic Surgery and Andrology, Mie University Graduate School of Medicine, Tsu, Mie, Japan

#Current Address: Department of Public Health Sciences, University of Chicago, Chicago, IL

Author Contributions

L.M.A. and S.W.H. designed research; L.M.A., T.S., O.F. performed research; L.M.A., L.W. and S.E.C. analyzed data; R.E.V. performed flow cytometry analysis; L.M.A., O.F., S.W.H. wrote the paper; and Y.J. contributed statistical expertise.

Disclosure statement: There are no conflicts of interest or affiliations to disclose.

array analysis revealed increased expression of cytokines and proteases such as LDLR, IL28 A/B, and MMP2 in diabetic mice.

Conclusion: Overall, NOD mice provide a model to examine the effects of hyperglycemia and chronic inflammation on the prostate, demonstrating relevance to some of the mechanisms present underlying BPH and potentially the initiation of prostate cancer.

Keywords

Non-Obese Diabetic Mice; Benign Prostatic Hyperplasia; Animal Model of BPH

Introduction:

Chronic inflammation is a key contributor in both the initiation and progression of a variety of diseases including arthritis, diabetes and various malignancies, affecting many organs including the prostate [1–3]. It has been hypothesized that prostatic inflammation may be a common contributory agent to both benign prostatic hyperplasia (BPH) and prostate cancer [4]. Histologically, BPH in humans is characterized by epithelial and stromal expansion in the prostate with the focal induction of new ductal architecture. Inflammation has been considered an important player in BPH [3] and has been associated with the severity of the disease [5]. Both the Reduction by Dutasteride of Prostate Cancer Events (REDUCE) and Medical Therapy of Prostatic Symptoms (MTOPS) studies linked histological prostatic inflammation with prostate enlargement and symptom scores [6,7]. Inflammatory comorbidities such as obesity, diabetes, and metabolic syndrome, are now recognized as playing an important role in BPH pathogenesis [8,9] and could potentially contribute to resistance in current medical therapies. However, it remains unclear whether these comorbidities result in overlapping or separate consequences and whether or how they affect BPH incidence or progression.

The structure of the human and mouse prostates differ greatly, with the human gland being an encapsulated compact organ while the mouse prostate has distinct lobes that grow outwards from the urethra [10]. Benign and malignant diseases are common in the human prostate, but the mouse organ is not normally a site for either hyperplasia or cancer. Although a series of *in vitro* and *in vivo* models have been developed and described as models of BPH [11], none of these fully recapitulates the pathobiology of the human condition. However, each model may shed light on specific aspects of the human disease. It is important to be able to determine the specific similarities between individual mouse models and human BPH to appropriately test aspects of disease biology and response to potential treatments. Most BPH patients suffer from multiple co-morbidities, often making it impractical to study these conditions individually in humans. Therefore, we used the non-obese diabetic (NOD) mouse model to better understand the role that inflammation and Type 1 diabetes in the absence of obesity play in the development of prostatic hyperplasia.

The NOD mouse is a stochastic model of Type 1 diabetes caused by autoimmune destruction of pancreatic β cells by T lymphocytes [12,13] which leads to the inhibition of insulin production. Diabetes in this model is characterized by insulitis and the onset of diabetes is indicated by a non-fasting glucose higher than 250 mg/dL along with glycosuria [14]. About

20–40% of male NOD mice develop diabetes between 12–30 weeks of age [15]. These inbred mice exhibit several abnormal immunophenotypes including defects in; the function of natural killer (NK) cells, cytokine production from macrophages, immunoregulatory function of antigen presenting cells, and in T-cell regulation [16]. To date, there have been few studies on the effects of autoimmunity on the prostate in these mice and none which focus on prostatic hyperplasia [17,18]. By using this model, we were able to study the effects of inflammation and diabetes individually, or in combination, on the mouse prostate to determine if there are any similarities to human BPH.

We observed the following: 1) Similar to human BPH, these mice displayed varying degrees of prostatic hyperplasia histologically characterized by epithelial hyperplasia and stromal expansion. 2) In addition, several diabetic mice displayed regions of prostatic intraepithelial neoplasia (PIN)-like changes in the prostate. 3) Both diabetic and non-diabetic mice showed increased inflammatory infiltrates in the prostate. 4) A panel of inflammatory or immune-related genes in diabetic mice was found to be associated with the degree of prostatic hyperplasia.

Materials and Methods:

Non-Obese Diabetic Mouse Model

Sixty 7-week-old male non-obese diabetic (NOD/ShiltJ) mice were purchased from Jackson Laboratory, Bar Harbor, ME (Stock Number: 001976). Mice were aged over the course of 32 weeks and were sacrificed at 26, 31, 34, 36, and 39 weeks old. Mice were injected with 100 mg/kg bromodeoxyuridine (BrdU) 20 minutes before being sacrificed using a CO_2 chamber. Serum was extracted immediately post-sacrifice and the prostate (all lobes), testes, seminal vesicles, bladder, kidney, liver, spleen, and pancreas were collected on ice. Tissues were formalin fixed and paraffin embedded or frozen in OCT.

Glucose Monitoring

Using a commercially available Contour glucose meter kit (Stock Number: 7151H) from Bayer AG (Whippany, NJ), non-fasting glucose readings were taken bi-weekly using blood collected via tail nick starting at 10 weeks old. Mice with readings above 250 mg/dL are considered to be diabetic while a reading above 400 mg/dL is considered severely diabetic [19].

Antibodies and Reagents

Antibodies and other reagents are listed in table 1. All antibodies were purchased directly from and validated by commercial vendors. For antibodies used in cell sorting normal splenic tissue was used to cross validate results.

Immunohistochemical and Histological Analysis

Mouse prostate tissues were fixed in 10% (v/v) formaldehyde in PBS, embedded in paraffin, and 5μm sections were cut. Sections were deparaffinized in xylene and rehydrated using gradient ethanol concentrations. For H&E staining, the sections were stained in Gill's III hematoxylin purchased from Sigma Aldrich (Stock Number: GHS316), for 7 min, washed in

running tap water for 5 min and quickly dipped in 1% acid alcohol. Slides were then rinsed in running tap water, dipped in saturated lithium carbonate to blue them and washed in running tap water for 1 min. Following this, slides were dipped in 95% alcohol and stained in eosin for 1 min. Finally, slides were dehydrated and mounted by routine methods.

Immunostaining was performed by using the Universal VECTASTAIN® Elite® ABC system following manufacturer's protocol. Slides were examined by a pathologist (SEC) and stromal hyperplasia and epithelial hyperplasia and piling were determined based upon these observations.

Statistical Analysis of Immunohistochemistry

Positively stained and unstained cells were counted manually in five high magnification fields of stained slides. Graphpad Prism version 7 for Windows, (GraphPad Software, La Jolla California USA, www.graphpad.com) was used to perform an unpaired t-test to determine whether samples differed significantly.

Scoring of Stromal Expansion

The area of stromal expansion in 100 sections of total glands, 50 sections from non-diabetic and 50 sections from diabetic mice was determined by measuring the total area of a single gland and then the stromal area using the ImageJ software. The measurement of stromal area was then divided by the total gland area to determine the percentage of stromal expansion.

Flow Cytometry

For each mouse, a part of the spleen was mechanically dissociated while one of each of the paired lobes of the prostate was digested in 1mg/mL collagenase I from Life Technologies, (Carlsband, CA) for up to one hour while shaking at 37° C. After digestion/dissociation, cell samples were washed and filtered before RBC removal. Cells were blocked with mouse Fc block (BD Pharmingen, 553142) and stained with Zombie Violet viability dye (Biolegend) followed by staining with antibodies to CD45 [30-F11], CD4[GK1.5], CD8[53–6.7], CD19[6D5], F4/80 [BM8], and CD11b[M1/70] according to the manufacturer's instructions (Biolegend). All samples were washed and filtered before flow analysis on a MACSQuant (Miltenyi). Final data analysis was conducted using FlowLogic software version 700.2A (Miltenyi). All cell events underwent debris and doublet exclusion followed by removal of dead cells containing Zombie Violet dye. The $CD45^+$ cells were gated on the viable cell population and the specific immune cell subsets were gated on the $CD45^+$ cell population. Three mice were analyzed for each group, where each point represents a single mouse.

Microarray Analysis and Cytokine Array

RNA was extracted from the anterior lobe of mouse prostates using a standard TRIzol extraction protocol and sent to the Genomics Facility at the University of Chicago where a Clariom S Affymetrix Gene Expression array for mice was conducted. The microarray data were processed and analyzed with R packages: "oligo"[20] for preprocessing, "limma"[21] for differentially expressed genes identification, and "EGSEA"[22] for gene set enrichment analyses with gene sets collected from GeneSetDB[23], KEGG[24], and MSigDB[25,26]. Cytokine detection was performed using Proteome Profiler Mouse XL Cytokine Array which detects

111 different analytes (R&D; ARY028). Analysis of the membranes acquired from the cytokine arrays was carried out by using the ImageJ software to analyze and quantify densitometric measurements.

Results:

NOD Mice Develop an Abnormal Prostate Hyperplasia

As in humans, where symptoms and histologic severity of prostatic enlargement vary by patient, we noticed variable histology in the NOD mouse model. When we analyzed prostatic tissues utilizing H&E staining, distinct histologic phenotypes were observed. We focused on analyzing the anterior prostate (AP) because this was the lobe that most prevalently displayed phenotypic changes. Other lobes appeared to largely maintain normal histology. Only one non-diabetic and one diabetic NOD mouse had AP lobes that appeared normal with intact glandular structures and normal cell composition. The remainder of the mice either had areas of epithelial piling and stromal expansion (Figure 1A). Even in the earliest time point tested (26 weeks), some degree of both epithelial piling and stromal expansion were observed in all mice, although in some animals foci of stromal expansion with no associated epithelial changes or of epithelial changes with no stromal expansion could also be found. From these samples it is not possible to say whether the stromal and epithelial expansion is concurrent or whether one precedes the other. After scoring the area of stromal expansion of 25 sections from each group, it was found that that there is an increase, though not significant in the areas analyzed, in stromal expansion in the diabetic mice (Figure 1B). Pathologic review suggests the presence of hyperplasia (increased cell numbers) rather than hypertrophy (increased cell size) in the stroma. This is consistent with the stromal expansion seen in human BPH.

Most non-diabetic mice had areas of focal hyperplasia and an increase in interstitial inflammation with focal lymphoid aggregates. These mice also exhibited areas with thickening of the basement membrane with smooth muscle adjacent. Diabetic mice exhibited marked stromal hyperplasia, abnormal gland clustering with an increase in mononuclear inflammation including lymphatic cells, macrophages and mast cells. The prostate epithelium in diabetic mice showed pleomorphic nuclei and an increase in the nuclear-to-cytoplasmic ratio. While both groups of mice had a similar percentage of mice with stromal expansion, non-diabetic mice were somewhat more likely to exhibit areas with epithelial piling (Figure 1C). BrdU staining revealed cell proliferation occurring in the stromal and epithelial tissues of both non-diabetic and diabetic mice, with an increase in areas of hyperplasia, especially in the diabetic NOD mice (Figure 1D). This finding could possibly indicate a metabolic mechanism contributing to the severity of hyperplasia.

Incidence of Diabetes in Male NOD Mice

Diabetes was observed as early as 18 weeks of age and the number of diabetic mice increased over time. About 48% of mice in our cohort became diabetic over the course of this study (supplemental Figure 1A). Out of twenty-nine diabetic mice, nineteen lost weight, and three suffered significant weight loss (>20% of the initial weight) and were euthanized prior to their scheduled termination. Only one mouse in the non-diabetic group lost weight

(supplemental figure 1B). A detailed table outlining the tag ID numbers of the mice, their diabetic status, change in weight, and histologic changes can be found in supplemental tables 1 and 2. Although a number of diabetic mice lost weight, four who became diabetic experienced either no significant decrease in weight or gained weight normally over the course of this study (supplemental table 2). To determine at what age prostatic phenotypes emerged, mice were sacrificed over a wide range of ages; 26, 31, 34, 36, and 39 weeks old.

Increased Immune Infiltration is Associated with a More Severe Prostatic Phenotype

Inherent immunodeficiencies in NOD mice have been well described. These mice suffer from the absence of circulating complement, which plays a role in antibody-mediated cytolysis [27], as well as a functional deficit in natural killer (NK) cells [28–30]. Furthermore, both antigen-presenting dendritic cells and macrophages in NOD mice exhibit maturation defects [31,32]. Although many studies have analyzed the function of the immune system in NOD mice, none have assessed the inflammatory profile of the prostate in these mice. Analysis of the prostate in NOD mice indeed supports alterations in inflammatory cell infiltrates of diabetic *versus* non-diabetic mice. Flow cytometry analysis of inflammatory infiltrates including T cells, B cells, and CD11b+ myeloid cells in NOD mice suggested increased inflammation in prostates of diabetic animals (supplemental figure 2). Analysis of three non-diabetic and three diabetic NOD mice demonstrated an increased trend of CD45+ cell infiltration and upward trend of CD8+ T cell and CD19+ B cell percentages within the immune compartment. The immune cell infiltrates within the spleens of these animals, however, remained unchanged. The alterations within the prostate were not significant, likely due to the low sample size. Therefore, we validated these findings within NOD mouse prostates using immunohistochemistry (IHC) to determine the presence of $CD4^+$ T-cells, $CD19^+$ B-cells, and $F4/80^+$ macrophages. These markers were chosen because in studies looking at inflammatory cells infiltrate in human BPH tissue, T-cells, B-cells, and macrophages were all shown to be commonly upregulated [33,34]. Positive staining of these markers was observed in both non-diabetic and diabetic mice (Figure 2A). Blind scoring revealed that diabetic NOD mice have an overall increase in these three cell types (Figure 2B) and also that leukocytes were more likely to invade the epithelial tissue in diabetic animals. Inflammation in non-diabetic mice appeared to be localized in interstitial tissues compared to diabetic mice where inflammation appeared to be more localized to glandular structures.

We found that epithelial hyperplasia was associated with inflammatory infiltrates in diabetic NOD mice even in the absence of stromal expansion in up to 29% vs. 7% of non-diabetic NOD mice. However, in the non-diabetic NOD mice stromal expansion was more frequently associated with inflammation (21%) compared to diabetic NOD mice (3%) (Figure 3). These data suggest that inflammation in diabetes could enhance the epithelial prostate phenotype observed in NOD mice.

We stained for androgen receptor expression in the male NOD mouse prostate and found positive staining in both non-diabetic and diabetic mice (Figure 4A). This expression was primarily found in epithelial cells but could also be seen in the stroma. In addition to this, IHC staining revealed NF-κB activation (Phospho-P65) in both groups of mice. Phospho-

P65 could be seen in the epithelial nuclei, some stromal nuclei, and within and adjacent to areas of inflammation (Figure 4B).

A Subset of Diabetic NOD Mice Develop Prostatic Intraepithelial Neoplasia

In addition to benign histologic changes we also observed potentially preneoplastic prostatic intraepithelial neoplasia (PIN)-like lesions (Figure 5A). In humans PIN is considered, by consensus, to be a precursor lesion to adenocarcinoma [35]. Two of the major characteristics of PIN are nuclear enlargement and an increased nuclear-to-cytoplasmic ratio. PIN-like changes were more common in the diabetic (8 out of 29 [27.6%]) than non-diabetic mice (3 out of 31 [9.7%]) within the anterior prostatic lobe (Figure 5A). The prostatic phenotypes in the diabetic mice with PIN-like changes (Dp) exhibited all histologic features observed in diabetic mice without PIN-like changes, however, in addition these mice also displayed nuclear atypia, nuclei with multiple nucleoli and an even greater increase in the nuclear-to-cytoplasmic ratio. Inflammatory cells in the prostate of Dp mice were more likely to infiltrate the basement membrane and were also more likely to sit close to PIN-like regions. Careful histologic examination of these lesions did not reveal and epithelial invasion into or through the basement membrane (Figure 5B). While cells undergoing mitosis could occasionally be identified, there appeared to be a loss of cell polarity, as well as, several apoptotic bodies and karyorrhectic nuclear debris in some areas. Furthermore, these mice exhibited highly proliferative luminal occlusion. Although continued investigation is required, this finding suggests that this model may also be useful in studying some early events leading towards prostate cancer.

c-Myc overexpression has been shown to induce PIN in transgenic mice [36,37] but no studies have looked at c-Myc expression in NOD mice in relation to PIN. Therefore, we used IHC to stain for c-Myc expression in PIN-like lesions. Cells in the stroma as well as the epithelium of the prostate expressed c-Myc with localization in both the nucleus and cytoplasm (Figure 5C). The specific role that c-Myc is playing in the onset or progression of prostatic hyperplasia in these mice remains unknown at this point.

Due to the presence of inflammatory cells and localization of c-Myc in the stroma and epithelium as well as the potentially pre-malignant PIN phenotype, we wanted to determine if there might be degradation of the extracellular matrix. MMP-2 and MMP-9 are enzymes associated with the degradation of collagen and other extracellular matrix proteins and play a role in cancer invasion and metastasis [38]. Both MMP-2 and MMP-9 have been shown to be potential prognostic markers of prostate cancer [39]. IHC staining revealed expression of both MMP-2 and MMP-9 throughout the prostate. (Figure 5D).

Diabetic NOD Mice Develop an Abnormal Testicular Phenotype

An abnormal testicular phenotype developed in diabetic mice, especially in mice with a more severe diabetic status indicated by a non-fasting blood glucose reading of 400 mg/dL and above [40]. While non-diabetic mice had completely normal testes, in the smaller testis recovered from the diabetic mice, the histopathology revealed a marked loss of tubules, vacuolization of the epithelial cells and dystrophic calcification (Figure 6A). The degree of testicular degradation varied but it was clear that a more severe diabetic status was

associated with increased degradation of the testes. Although prostatic hyperplasia was present in the mice, testicular degeneration was also associated with shrinkage of the whole prostatic complex and seminal vesicles (Figure 6B) reminiscent of the gross phenotype of the genital tract of a castrated male mouse.

The histology of the pancreas in these mice was also analyzed. In non-diabetic NOD mice, microscopic sections of the pancreas (supplemental figure 3A) revealed the presence of islet cells surrounded by mononuclear inflammatory cells. In some areas, the inflammatory infiltrate invaded into the islet cell mass and was associated with pyknotic nuclei and apoptotic-appearing bodies. The acinar component exhibited focal vacuolization and variability in the nuclear-to-cytoplasmic ratio. Unlike the non-diabetic NOD mice, the islet cell mass was markedly reduced or absent in the diabetic NOD mice. In those cases where residual islets were observed, there was an increase in pyknotic and apoptotic-appearing cells. Mononuclear infiltrates were scattered throughout the pancreatic tissue. The ducts showed dilation occasional staghorn-type morphology. Vacuolization within the exocrine component of the organ was more abundant than the non-diabetic group. In the subset of animals demonstrating PIN-like histology, inflammatory cells were often found to directly invade the islets and vacuole density was higher than other groups. Scoring of the pancreatic structures can be found in supplemental figure 3B. These observations suggest that as mice age the inflammatory processes that cause diabetes do not stop, merely that they strike different mice at different ages.

Microarray Analysis Reveals Differentially Expressed Genes in Diabetic Mice with PIN-Like Changes vs. Non-Diabetic Mice

We utilized the Clariom S Mouse Affymetrix microarray system to determine which genes and gene sets are upregulated in the anterior prostate of these mice. The anterior prostate was chosen because it was in this prostatic lobe that the most significant phenotypic changes were observed (Figure 1). Using Gene Set Enrichment Analysis (GSEA) we were able to determine differentially expressed genes (DEG) between diabetic (Di), non-diabetic (ND) mice and diabetic with PIN-like changes (Dp). We found that there was only one DEG (*Uts2b*) when comparing Di vs ND and five DEGs were observed between Dp vs Di, all were upregulated in Di mice (Figure 7A). Interestingly, when comparing Dp vs ND, there were 67 DEGs, 34 of which were upregulated in Dp mice. (Figure 7B). 13 of these upregulated DEGs (highlighted in Figure 7B) are involved in inflammatory or immune-related processes. A table with a full list of DEGs in Dp vs ND mice can be found is supplemental figure 4A. Work has been done in humans that links a few of the genes found to be upregulated in Dp mice to BPH and/or cancer [41–44].

Cytokine Array Analysis

NOD mice exhibit multiple aberrant immunophenotypes, including cytokine deregulation that may contribute to the observed prostate changes. To gain a better understanding of which cytokines are up- or down-regulated in the prostates of non-diabetic vs. diabetic mice, we performed a cytokine array to assess the levels of over 100 cytokines, chemokines and proteases using the Proteome Profiler Mouse XL kit. The anterior prostates, from mice without PIN lesions, were used because, as previously stated, the most significant

histopathologic changes occurred in this lobe and only a small subset of mice developed PIN lesions. The relative expression of the secreted factors was analyzed by densitometry using the desktop application Image J. Of the 111 analytes, seven were significantly upregulated in diabetic NOD mice (Figure 7C). This included coagulation factor III/ tissue factor (TF/ CD142), flt-3 ligand (Flt3lg), IL 28A/B, low density lipoprotein receptor (LDLR), leukemia inhibitory factor (LIF), and lipocallin-2/NGAL (LCN2). In addition to these upregulated analytes, and consistent with our analysis, MMP-2 was also among the analytes found to be upregulated in diabetic mice. Whole cytokine array membranes can be found in supplemental figure 4B.

Discussion:

In humans, BPH is characterized by the nodular, nonmalignant proliferation of epithelial and/or stromal cells, resulting in focal development of new glandular structures, predominantly within the transition zone of the prostate [45,46]. Classical descriptions suggested that stromal nodules develop first and that epithelial structures subsequently invade and arborize. However, McNeal showed that, while such stromal nodules are common in the periurethral prostate, in the transition zone the nodules appear to be glandular from their inception [47,48] suggesting that both epithelial and stromal proliferation are important components of human BPH. It is important to note that in humans while there is proliferation of both epithelial and stromal cells the result is new ductal architecture that is histologically normal, making detection in needle biopsies difficult, and that BPH is recognized by the pattern of growth and focal expansion rather than by abnormal local histology.

Mouse models are important components in the development and testing of therapeutic interventions for many diseases. In the case of BPH, none of the available mice reflect all aspects of the disease as it occurs in humans. This makes it important to examine individual models critically to determine how they can best contribute insights to the human condition. In humans BPH, often causes compression of the urethra, and is a well-recognized cause of lower urinary tract symptoms (LUTS), a symptomatic syndrome that includes frequency and urgency to urinate, nocturia, and weak urine stream [45,46,49]. The prostates of rodents are composed of lobes that, in general, are not closely associated with the urethra. Therefore, their expansion is not a cause of urinary retention. An exception to this generalization is the new growth of prostatic ductal tissue within the rhabdosphincter that can be elicited by sex steroid hormones and has been shown to cause urethral compression in both rats [50] and mice [51]. It is worth noting that the rhabdosphincter is relatively much thicker and more developed in rodents than in humans [52], so even this apparent similarity in growth and functional outcome is not truly equivalent to the human condition.

We showed here that NOD mice replicate certain key features of prostatic hyperplasia including stromal and epithelial proliferation and associated inflammation. The several prostate phenotypes observed in NOD mice mimic to a certain extent the ones observed in patients with benign prostate hyperplasia. Regardless of diabetic status these mice displayed histologic changes in their prostates. We observed areas of hyperplasia in these mice as early as 26 weeks of age and the severity of hyperplasia increased with both age and diabetic

status, similar to what is observed in human BPH patients. BPH in humans is a focal enlargement usually centered in the transition zone of the prostate, adjacent to the prostatic urethra. In NOD mice we saw lobe specific effects with the greatest stromal and epithelial proliferation seen in the anterior prostate. While we were able to observe these changes in the prostate, currently it is unclear if stromal expansion precedes epithelial hyperplasia or vice versa. There is no correlation between mouse prostate lobes and the zones of the human prostate [53] so the regional nature of human BPH is not truly recapitulated in mouse models. In addition the prostatic expansion seen in mouse models, including this one, is not an exact histologic match for that seen in humans, where BPH is, in essence, an amplification of normal transitional zone architecture. In contrast the epithelial hyperplasia seen in the mouse represented more piling of cells than in humans.

Inflammation and inflammatory comorbidities such as diabetes and obesity are associated with the progression of BPH to therapy resistance and ultimately to surgery. Obese men tend to suffer more from obstruction due to an enlarged prostate, and also tend to be more resistant to 5α-reductase inhibitor (5ARI) treatment [54,55]. Larger prostate volumes were found in patients suffering from LUTS and type 2 diabetes compared to patients suffering from LUTS who did not have type 2 diabetes [56]. Diabetics with higher prostate volumes and PSA levels are more likely to report more severe LUTS with the duration of diabetes being associated with symptom severity [55,57]. Although BPH patients usually suffer from type 2 diabetes, where the amount of insulin produced by the pancreas does not meet the needs of the body or the body's cells are resistant to the produced insulin, BPH has been considered to potentially have an autoimmune component [33,58]. Many human BPH studies have shown an upregulation in various inflammatory infiltrates including T-cells, B-cells and macrophages. Notably, Theyer *et al* stated that compared to normal tissues, up to 60% of T-cells in BPH tissues were found to be $CD4^+$ [34] . Here we show a similar pattern of increased B-cells, CD4+ T-cells, CD8+-T cells and F4/80+ macrophages in the prostate of the NOD mouse using IHC. These data suggest that prostatic inflammation is exacerbated by diabetes in this model. This mouse has been characterized as a model for autoimmune diseases such as type 1 diabetes and has also been used as a model of inflammatory prostatitis [17,18,59–62]. Unlike humans where patients suffering from type 2 diabetes tend have larger prostates, the prostates in diabetic NOD mice were smaller compared to non-diabetic mice, reflecting histologic changes to the testes secondary to type 1 diabetes. However, histologically these mice still exhibited focally-increased proliferation of epithelial and stromal cells.

Observations in the pancreas, demonstrate that autoimmune destruction of islet cells occurs at all ages and therefore the proportion of diabetic mice increases with age. Many studies have demonstrated that diabetes in animal models and humans interferes with spermatogenesis and can affect fertility [63,64]. Schoeller et al. concluded that low levels of insulin due to type 1 diabetes leads to a disruption in the hypothalamic pituitary gonadal axis. This disruption subsequently causes a decrease in follicle-stimulating hormone (FSH) and luteinizing hormone (LH) signaling to the testes which in turn negatively impacts spermatogenesis. Testicular atrophy has been observed in diabetic Akita mice, as well as, diabetic BB Wistar rat [64,65]. Akita mice express a mutant, nonfunctional form of insulin II (*ins2*) in the testes and pancreas. Male Akita homozygous mice were shown to be infertile and have abnormal testicular morphology and reduced testis size [65]. The BB Wistar rat

spontaneously develops diabetes and demonstrates testicular atrophy occurring as early as 121 days old with increasing severity as the rats age [64]. There have been studies of the testicular alterations in NOD mice [66], however, none have analyzed the associations of these alterations with prostatic hyperplasia. We have shown that regardless of testicular status, NOD mice develop regions of prostatic hyperplasia within the anterior lobe.

The observation of hyperplasia, even in mice with shrunken and/or dysfunctional testes is indicative that androgens may not be required for continued cellular proliferation in these mice. In humans, many BPH patients fail 5ARI therapy, especially those patients with inflamed prostates. In these patients, the hyperplastic prostate continues to grow even though there is an inhibition in the conversion of testosterone to DHT, which can be monitored by decreases in the expression of the androgen-dependent protein PSA [67]. This indicates that there are alternative mechanisms leading to BPH progression. Tissue samples taken from BPH patients whose disease progressed to surgery expressed significantly higher androgen receptor and androgen receptor variant 7 as well as SRD5A2 levels when compared to patients with earlier stage disease and low symptom scores. Furthermore, activation of NF-κB is associated with inflammation, as seen in advanced BPH, and led to upregulation of these same genes, linking inflammation to androgen synthesis and signaling [68,69]. It is possible that inflammation in the NOD mouse may be providing a similar mechanism to support prostate growth, sidestepping the loss of testicular function.

c-Myc is a transcription factor that plays an important role in regulating cell division and can inhibit the expression of genes with antiproliferative functions [70]. c-Myc has been shown to have several roles in the NOD model such as causing resistance to glucocorticoid-induced apoptosis [71]. We show here that diabetic NOD mice develop focal PIN-like changes. This observation, taken along with the finding of c-Myc expression in these foci, is consistent with the myc activation seen in human prostate adenocarcinoma. The role that c-Myc plays in the causation or progression of the prostatic phenotype seen in NOD mice is unknown, it may potentially be involved in the increase in cell proliferation observed in the diabetic NOD mice, especially those with PIN lesions. Several of the upregulated cytokines identified including tissue factor[72–74], LDLR[75,76], LIF[77,78] and LCN2[79-81] have been implicated in cancer cell proliferation or cancer progression while Flt3-ligand has potential for use in immunotherapy[82–84]. While this is the case, the role(s) that these cytokines are playing in the context of the NOD mouse model and/or BPH is poorly understood. The indication(s) of the majority of the DEGs upregulated in Dp mice is still unknown, however, some work has been done on CCL3 and TNFSF10 [41–43] in humans. For example, Tyagi et. al has shown association of increased urine levels of a number of chemokines and cytokines including CCL3 with prostatic tissue inflammation score and lymphocytic infiltration in human BPH patients [44]. Furthermore, CCL3 has been shown to be a key player in the AR-CCL3 dependent pathway used by macrophages to induce stromal proliferation [85]. Further studies are needed to elucidate the role, if any, that the differentially expressed genes from the microarray and upregulated analytes from the cytokine array have in the NOD mouse, BPH and/or PIN.

Our studies illustrate the utility of the NOD mouse in the study of some aspects of various prostatic conditions, including prostatic hyperplasia and potentially the initiation of prostate

cancer. Since many human BPH patients suffer from multiple diseases at once, it is difficult to study the effects that individual diseases have on BPH causation or progression. Currently, a significant number of BPH patients become resistant to therapy leading to around 120,000 surgical interventions annually in the United States [86]. The role of inflammatory comorbidities in the progression of human BPH make this model of immune-initiated hyperplasia potentially useful in testing therapies aimed at this aspect of the disease.

Supplementary Material

Refer to Web version on PubMed Central for supplementary material.

Acknowledgements

This work was supported by the taxpayers of the United States through NIH grants DK111186 (to L.M.A.), DK103483 and DK117906 (to S.W.H.). We also gratefully acknowledge the support of William and Judith Davis as well as the Rob Brooks Fund for Precision Prostate Cancer Care, created by many donors, in making this project possible.

Abbreviations

BPH	Benign prostatic hyperplasia
NOD Mice	Non-obese Diabetic Mice
GSEA	Gene Set Enrichment Analysis
DEGs	Differentially Expressed Genes
ND	Non-diabetic NOD mice
Di	Diabetic NOD mice
Dp	Diabetic NOD mice with PIN-like changes

References:

1. Esser N, Legrand-Poels S, Piette J, Scheen AJ, Paquot N. Inflammation as a link between obesity, metabolic syndrome and type 2 diabetes. Diabetes Res Clin Pract. 2014;105(2):141–150. [PubMed: 24798950]
2. Greenwald RA. Oxygen radicals, inflammation, and arthritis: pathophysiological considerations and implications for treatment. Semin Arthritis Rheum. 1991;20(4):219–240. [PubMed: 2042055]
3. Robert G, Descazeaud A, Nicolaiew N, et al. Inflammation in benign prostatic hyperplasia: a 282 patients' immunohistochemical analysis. Prostate. 2009;69(16):1774–1780. [PubMed: 19670242]
4. De Nunzio C, Kramer G, Marberger M, et al. The controversial relationship between benign prostatic hyperplasia and prostate cancer: the role of inflammation. Eur Urol. 2011;60(1):106–117. [PubMed: 21497433]
5. Wang L, Yang JR, Yang LY, Liu ZT. Chronic inflammation in benign prostatic hyperplasia: implications for therapy. Med Hypotheses. 2008;70(5):1021–1023. [PubMed: 17935901]
6. Nickel JC, Roehrborn CG, O'Leary MP, Bostwick DG, Somerville MC, Rittmaster RS. The relationship between prostate inflammation and lower urinary tract symptoms: examination of baseline data from the REDUCE trial. Eur Urol. 2008;54(6):1379–1384. [PubMed: 18036719]

7. Roehrborn CG, Kaplan SA, Noble WD, Lucia MS, Slawin KMM, K.T., al. e. The impact of acute or chronic inflammation in baseline biopsy on the risk of clinical progression of BPH: results from the MTOPS study. J Urol. 2005;173(Suppl)(346).
8. Jiang M, Strand DW, Franco OE, Clark PE, Hayward SW. PPARgamma: a molecular link between systemic metabolic disease and benign prostate hyperplasia. Differentiation. 2011;82(4–5):220–236. [PubMed: 21645960]
9. Fowke JH, Koyama T, Fadare O, Clark PE. Does Inflammation Mediate the Obesity and BPH Relationship? An Epidemiologic Analysis of Body Composition and Inflammatory Markers in Blood, Urine, and Prostate Tissue, and the Relationship with Prostate Enlargement and Lower Urinary Tract Symptoms. PLoS ONE. 2016;11(6):e0156918. [PubMed: 27336586]
10. Aaron L, Franco OE, Hayward SW. Review of Prostate Anatomy and Embryology and the Etiology of Benign Prostatic Hyperplasia. Urol Clin North Am. 2016;43(3):279–288. [PubMed: 27476121]
11. Mahapokai W, Van Sluijs FJ, Schalken JA. Models for studying benign prostatic hyperplasia. Prostate Cancer Prostatic Dis. 2000;3(1):28–33. [PubMed: 12497158]
12. Castano L, Eisenbarth GS. Type-I diabetes: a chronic autoimmune disease of human, mouse, and rat. Annu Rev Immunol. 1990;8:647–679. [PubMed: 2188676]
13. Kikutani H, Makino S. The murine autoimmune diabetes model: NOD and related strains. Adv Immunol. 1992;51:285–322. [PubMed: 1323922]
14. Han BG, Hao CM, Tchekneva EE, et al. Markers of glycemic control in the mouse: comparisons of 6-h- and overnight-fasted blood glucoses to Hb A1c. Am J Physiol Endocrinol Metab. 2008;295(4):E981–986. [PubMed: 18664598]
15. Cechin SR, Lopez-Ocejo O, Karpinsky-Semper D, Buchwald P. Biphasic decline of beta-cell function with age in euglycemic nonobese diabetic mice parallels diabetes onset. IUBMB Life. 2015;67(8):634–644. [PubMed: 26099053]
16. Fan H, Longacre A, Meng F, et al. Cytokine dysregulation induced by apoptotic cells is a shared characteristic of macrophages from nonobese diabetic and systemic lupus erythematosus-prone mice. J Immunol. 2004;172(8):4834–4843. [PubMed: 15067061]
17. Penna G, Amuchastegui S, Cossetti C, et al. Treatment of experimental autoimmune prostatitis in nonobese diabetic mice by the vitamin D receptor agonist elocalcitol. J Immunol. 2006;177(12): 8504–8511. [PubMed: 17142748]
18. Rivero VE, Cailleau C, Depiante-Depaoli M, Riera CM, Carnaud C. Non-obese diabetic (NOD) mice are genetically susceptible to experimental autoimmune prostatitis (EAP). J Autoimmun. 1998;11(6):603–610. [PubMed: 9878082]
19. Li X, Kaminski NE, Fischer LJ. Examination of the immunosuppressive effect of delta9-tetrahydrocannabinol in streptozotocin-induced autoimmune diabetes. Int Immunopharmacol. 2001;1(4):699–712. [PubMed: 11357882]
20. Carvalho BS, Irizarry RA. A framework for oligonucleotide microarray preprocessing. Bioinformatics. 2010;26(19):2363–2367. [PubMed: 20688976]
21. Ritchie ME, Phipson B, Wu D, et al. limma powers differential expression analyses for RNA-sequencing and microarray studies. Nucleic Acids Res. 2015;43(7):e47. [PubMed: 25605792]
22. Alhamdoosh M, Ng M, Wilson NJ, et al. Combining multiple tools outperforms individual methods in gene set enrichment analyses. Bioinformatics. 2017;33(3):414–424. [PubMed: 27694195]
23. Araki H, Knapp C, Tsai P, Print C. GeneSetDB: A comprehensive meta-database, statistical and visualisation framework for gene set analysis. FEBS Open Bio. 2012;2:76–82.
24. Kanehisa M, Sato Y, Kawashima M, Furumichi M, Tanabe M. KEGG as a reference resource for gene and protein annotation. Nucleic Acids Res. 2016;44(D1):D457–462. [PubMed: 26476454]
25. Liberzon A, Birger C, Thorvaldsdottir H, Ghandi M, Mesirov JP, Tamayo P. The Molecular Signatures Database (MSigDB) hallmark gene set collection. Cell Syst. 2015;1(6):417–425. [PubMed: 26771021]
26. Subramanian A, Tamayo P, Mootha VK, et al. Gene set enrichment analysis: a knowledge-based approach for interpreting genome-wide expression profiles. Proc Natl Acad Sci U S A. 2005;102(43):15545–15550. [PubMed: 16199517]

27. Lewis EJ. Patterns of circulating complement in renal diseases. Annu Rev Med. 1979;30:445–455. [PubMed: 400505]
28. Baxter AG, Cooke A. Complement lytic activity has no role in the pathogenesis of autoimmune diabetes in NOD mice. Diabetes. 1993;42(11):1574–1578. [PubMed: 8405697]
29. Kataoka S, Satoh J, Fujiya H, et al. Immunologic aspects of the nonobese diabetic (NOD) mouse. Abnormalities of cellular immunity. Diabetes. 1983;32(3):247–253. [PubMed: 6298042]
30. Serreze DV, Leiter EH. Defective activation of T suppressor cell function in nonobese diabetic mice. Potential relation to cytokine deficiencies. J Immunol. 1988;140(11):3801–3807. [PubMed: 2897395]
31. Pearson T, Markees TG, Serreze DV, et al. Genetic disassociation of autoimmunity and resistance to costimulation blockade-induced transplantation tolerance in nonobese diabetic mice. J Immunol. 2003;171(1):185–195. [PubMed: 12816997]
32. Serreze DV, Gaedeke JW, Leiter EH. Hematopoietic stem-cell defects underlying abnormal macrophage development and maturation in NOD/Lt mice: defective regulation of cytokine receptors and protein kinase C. Proc Natl Acad Sci U S A. 1993;90(20):9625–9629. [PubMed: 8415751]
33. Kramer G, Mitteregger D, Marberger M. Is benign prostatic hyperplasia (BPH) an immune inflammatory disease? Eur Urol. 2007;51(5):1202–1216. [PubMed: 17182170]
34. Theyer G, Kramer G, Assmann I, et al. Phenotypic characterization of infiltrating leukocytes in benign prostatic hyperplasia. Lab Invest. 1992;66(1):96–107. [PubMed: 1370561]
35. Brawer MK. Prostatic intraepithelial neoplasia: an overview. Rev Urol. 2005;7 Suppl 3:S11–18.
36. Iwata T, Schultz D, Hicks J, et al. MYC overexpression induces prostatic intraepithelial neoplasia and loss of Nkx3.1 in mouse luminal epithelial cells. PLoS One. 2010;5(2):e9427. [PubMed: 20195545]
37. Zhang X, Lee C, Ng PY, Rubin M, Shabsigh A, Buttyan R. Prostatic neoplasia in transgenic mice with prostate-directed overexpression of the c-myc oncoprotein. Prostate. 2000;43(4):278–285. [PubMed: 10861747]
38. Zhang L, Shi J, Feng J, Klocker H, Lee C, Zhang J. Type IV collagenase (matrix metalloproteinase-2 and −9) in prostate cancer. Prostate Cancer Prostatic Dis. 2004;7(4):327–332. [PubMed: 15356679]
39. Morgia G, Falsaperla M, Malaponte G, et al. Matrix metalloproteinases as diagnostic (MMP-13) and prognostic (MMP-2, MMP-9) markers of prostate cancer. Urol Res. 2005;33(1):44–50. [PubMed: 15517230]
40. Guo TL, Germolec DR, Zheng JF, et al. Genistein protects female nonobese diabetic mice from developing type 1 diabetes when fed a soy- and alfalfa-free diet. Toxicol Pathol. 2015;43(3):435–448. [PubMed: 24713318]
41. He W, Wang Q, Xu J, et al. Attenuation of TNFSF10/TRAIL-induced apoptosis by an autophagic survival pathway involving TRAF2- and RIPK1/RIP1-mediated MAPK8/JNK activation. Autophagy. 2012;8(12):1811–1821. [PubMed: 23051914]
42. Hod Y Differential control of apoptosis by DJ-1 in prostate benign and cancer cells. J Cell Biochem. 2004;92(6):1221–1233. [PubMed: 15258905]
43. Micheau O, Shirley S, Dufour F. Death receptors as targets in cancer. Br J Pharmacol. 2013;169(8):1723–1744. [PubMed: 23638798]
44. Tyagi P, Motley SS, Koyama T, et al. Molecular correlates in urine for the obesity and prostatic inflammation of BPH/LUTS patients. Prostate. 2018;78(1):17–24. [PubMed: 29080225]
45. McNeal JE. Origin and evolution of benign prostatic enlargement. Invest Urol. 1978;15(4):340–345. [PubMed: 75197]
46. McVary KT. BPH: epidemiology and comorbidities. Am J Manag Care. 2006;12(5 Suppl):S122–128. [PubMed: 16613526]
47. McNeal JE. Relationship of the Origin of Benign Prostatic Hypertrophy to Prostatic Structure of Man and Other Mammals In: Hinman F, Boyarsky S, eds. Benign Prostatic Hypertrophy. New York, NY: Springer New York; 1983:152–166.
48. McNeal JE. The prostate gland: morphology and pathobiology. Monogr Urology. 1988(4):3–37.

49. Wei JT, Calhoun E, Jacobsen SJ. Urologic diseases in America project: benign prostatic hyperplasia. J Urol. 2005;173(4):1256–1261. [PubMed: 15758764]
50. Bernoulli J, Yatkin E, Konkol Y, Talvitie EM, Santti R, Streng T. Prostatic inflammation and obstructive voiding in the adult Noble rat: impact of the testosterone to estradiol ratio in serum. Prostate. 2008;68(12):1296–1306. [PubMed: 18500685]
51. Nicholson TM, Ricke EA, Marker PC, et al. Testosterone and 17beta-estradiol induce glandular prostatic growth, bladder outlet obstruction, and voiding dysfunction in male mice. Endocrinology. 2012;153(11):5556–5565. [PubMed: 22948219]
52. Cunha GR, Vezina CM, Isaacson D, et al. Development of the human prostate. Differentiation. 2018;103:24–45. [PubMed: 30224091]
53. Shappell SB, Thomas GV, Roberts RL, et al. Prostate pathology of genetically engineered mice: definitions and classification. The consensus report from the Bar Harbor meeting of the Mouse Models of Human Cancer Consortium Prostate Pathology Committee. Cancer Res. 2004;64(6): 2270–2305. [PubMed: 15026373]
54. Parsons JK, Sarma AV, McVary K, Wei JT. Obesity and benign prostatic hyperplasia: clinical connections, emerging etiological paradigms and future directions. J Urol. 2009;182(6 Suppl):S27–31. [PubMed: 19846130]
55. Qu X, Huang Z, Meng X, Zhang X, Dong L, Zhao X. Prostate volume correlates with diabetes in elderly benign prostatic hyperplasia patients. Int Urol Nephrol. 2014;46(3):499–504. [PubMed: 24022843]
56. Hammarsten J, Hogstedt B, Holthuis N, Mellstrom D. Components of the metabolic syndrome-risk factors for the development of benign prostatic hyperplasia. Prostate Cancer Prostatic Dis. 1998;1(3):157–162. [PubMed: 12496910]
57. Van Den Eeden SK, Ferrara A, Shan J, et al. Impact of type 2 diabetes on lower urinary tract symptoms in men: a cohort study. BMC Urol. 2013;13:12. [PubMed: 23421436]
58. Chughtai B, Lee R, Te A, Kaplan S. Role of inflammation in benign prostatic hyperplasia. Rev Urol. 2011;13(3):147–150. [PubMed: 22110398]
59. Atkinson MA, Leiter EH. The NOD mouse model of type 1 diabetes: as good as it gets? Nat Med. 1999;5(6):601–604. [PubMed: 10371488]
60. King C, Sarvetnick N. The incidence of type-1 diabetes in NOD mice is modulated by restricted flora not germ-free conditions. PLoS One. 2011;6(2):e17049. [PubMed: 21364875]
61. Pearson JA, Wong FS, Wen L. The importance of the Non Obese Diabetic (NOD) mouse model in autoimmune diabetes. J Autoimmun. 2016;66:76–88. [PubMed: 26403950]
62. Jackson CM, Flies DB, Mosse CA, Parwani A, Hipkiss EL, Drake CG. Strain-specific induction of experimental autoimmune prostatitis (EAP) in mice. Prostate. 2013;73(6):651–656. [PubMed: 23129407]
63. Schoeller EL, Schon S, Moley KH. The effects of type 1 diabetes on the hypothalamic, pituitary and testes axis. Cell Tissue Res. 2012;349(3):839–847. [PubMed: 22526620]
64. Wright JR Jr., Yates AJ, Sharma HM, Shim C, Tigner RL, Thibert P. Testicular atrophy in the spontaneously diabetic BB Wistar rat. Am J Pathol. 1982;108(1):72–79. [PubMed: 7091303]
65. Schoeller EL, Albanna G, Frolova AI, Moley KH. Insulin rescues impaired spermatogenesis via the hypothalamic-pituitary-gonadal axis in Akita diabetic mice and restores male fertility. Diabetes. 2012;61(7):1869–1878. [PubMed: 22522616]
66. Gondos B, Bevier W. Effect of insulin on testicular alterations in the nonobese diabetic mouse. Ann Clin Lab Sci. 1995;25(3):272–277. [PubMed: 7605110]
67. Lin-Tsai O, Clark PE, Miller NL, et al. Surgical intervention for symptomatic benign prostatic hyperplasia is correlated with expression of the AP-1 transcription factor network. Prostate. 2014;74(6):669–679. [PubMed: 24500928]
68. Austin DC, Strand DW, Love HL, et al. NF-kappaB and androgen receptor variant 7 induce expression of SRD5A isoforms and confer 5ARI resistance. Prostate. 2016;76(11):1004–1018. [PubMed: 27197599]
69. Austin DC, Strand DW, Love HL, et al. NF-kappaB and androgen receptor variant expression correlate with human BPH progression. Prostate. 2016;76(5):491–511. [PubMed: 26709083]

70. Miller DM, Thomas SD, Islam A, Muench D, Sedoris K. c-Myc and cancer metabolism. Clin Cancer Res. 2012;18(20):5546–5553. [PubMed: 23071356]
71. Martins TC, Aguas AP. Involvement of c-myc in the resistance of non-obese diabetic mice to glucocorticoid-induced apoptosis. Immunology. 1998;95(3):377–382. [PubMed: 9824500]
72. Akashi T, Furuya Y, Ohta S, Fuse H. Tissue factor expression and prognosis in patients with metastatic prostate cancer. Urology. 2003;62(6):1078–1082. [PubMed: 14665359]
73. Kaushal V, Mukunyadzi P, Siegel ER, Dennis RA, Johnson DE, Kohli M. Expression of tissue factor in prostate cancer correlates with malignant phenotype. Appl Immunohistochem Mol Morphol. 2008;16(1):1–6. [PubMed: 18091328]
74. Ruf W, Yokota N, Schaffner F. Tissue factor in cancer progression and angiogenesis. Thromb Res. 2010;125 Suppl 2:S36–38. [PubMed: 20434002]
75. Chen Y, Hughes-Fulford M. Human prostate cancer cells lack feedback regulation of low-density lipoprotein receptor and its regulator, SREBP2. Int J Cancer. 2001;91(1):41–45. [PubMed: 11149418]
76. Furuya Y, Sekine Y, Kato H, Miyazawa Y, Koike H, Suzuki K. Low-density lipoprotein receptors play an important role in the inhibition of prostate cancer cell proliferation by statins. Prostate Int. 2016;4(2):56–60. [PubMed: 27358845]
77. Kellokumpu-Lehtinen P, Talpaz M, Harris D, Van Q, Kurzrock R, Estrov Z. Leukemia-inhibitory factor stimulates breast, kidney and prostate cancer cell proliferation by paracrine and autocrine pathways. Int J Cancer. 1996;66(4):515–519. [PubMed: 8635867]
78. Zeng H, Qu J, Jin N, et al. Feedback Activation of Leukemia Inhibitory Factor Receptor Limits Response to Histone Deacetylase Inhibitors in Breast Cancer. Cancer Cell. 2016;30(3):459–473. [PubMed: 27622335]
79. Ding G, Wang J, Feng C, Jiang H, Xu J, Ding Q. Lipocalin 2 over-expression facilitates progress of castration-resistant prostate cancer via improving androgen receptor transcriptional activity. Oncotarget. 2016;7(39):64309–64317. [PubMed: 27602760]
80. Mahadevan NR, Rodvold J, Almanza G, Perez AF, Wheeler MC, Zanetti M. ER stress drives Lipocalin 2 upregulation in prostate cancer cells in an NF-kappaB-dependent manner. BMC Cancer. 2011;11:229. [PubMed: 21649922]
81. Tung MC, Hsieh SC, Yang SF, et al. Knockdown of lipocalin-2 suppresses the growth and invasion of prostate cancer cells. Prostate. 2013;73(12):1281–1290. [PubMed: 23775308]
82. Ciavarra RP, Somers KD, Brown RR, et al. Flt3-ligand induces transient tumor regression in an ectopic treatment model of major histocompatibility complex-negative prostate cancer. Cancer Res. 2000;60(8):2081–2084. [PubMed: 10786663]
83. Curran MA, Allison JP. Tumor vaccines expressing flt3 ligand synergize with ctla-4 blockade to reject preimplanted tumors. Cancer Res. 2009;69(19):7747–7755. [PubMed: 19738077]
84. Lynch DH, Andreasen A, Maraskovsky E, Whitmore J, Miller RE, Schuh JC. Flt3 ligand induces tumor regression and antitumor immune responses in vivo. Nat Med. 1997;3(6):625–631. [PubMed: 9176488]
85. Wang X, Lin WJ, Izumi K, et al. Increased infiltrated macrophages in benign prostatic hyperplasia (BPH): role of stromal androgen receptor in macrophage-induced prostate stromal cell proliferation. J Biol Chem. 2012;287(22):18376–18385. [PubMed: 22474290]
86. Lytton B, Emery JM, Harvard BM. The incidence of benign prostatic obstruction. J Urol. 1968;99(5):639–645. [PubMed: 4171950]

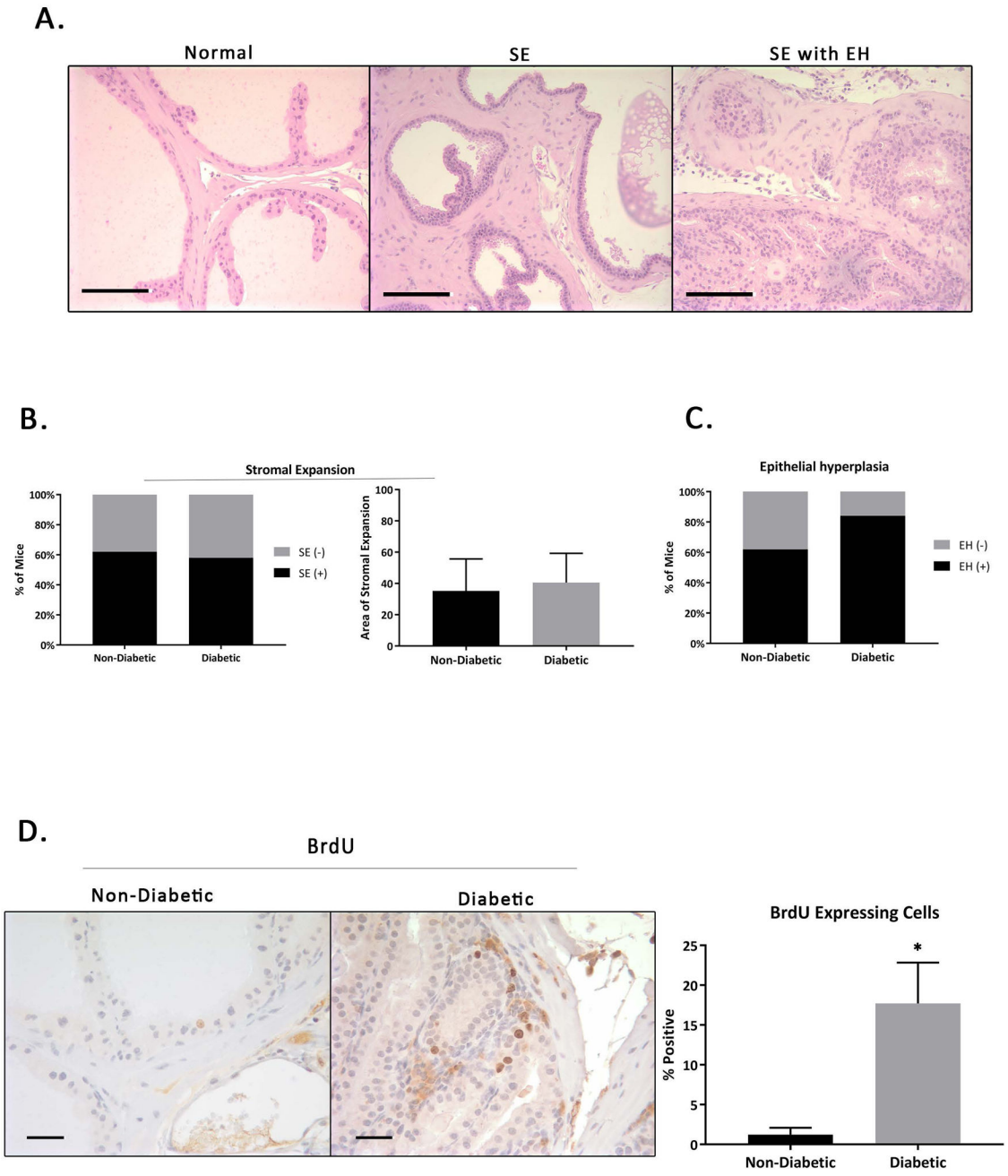

Figure 1. Histologic Changes in the Male NOD Mouse Prostate

A) NOD mice exhibit a range of prostatic phenotypes including areas that have normal prostatic composition, areas of stromal expansion (SE) and areas that have both SE and epithelial hyperplasia (EH). **B)** The first graph shows percentage of mice with stromal expansion. The second graph shows the average area of stromal expansion as a percentage of the total measured area non-diabetic compared to diabetic mice. **C)** Percentage of mice with epithelial hyperplasia. While both non-diabetic and diabetic mice experience a similar percentage of stromal expansion, diabetic mice were more likely to exhibit epithelial

hyperplasia. **D)** Immunohistochemical staining of BrdU in diabetic and non-diabetic male NOD mice reveals increased epithelial proliferation in diabetic NOD mice.

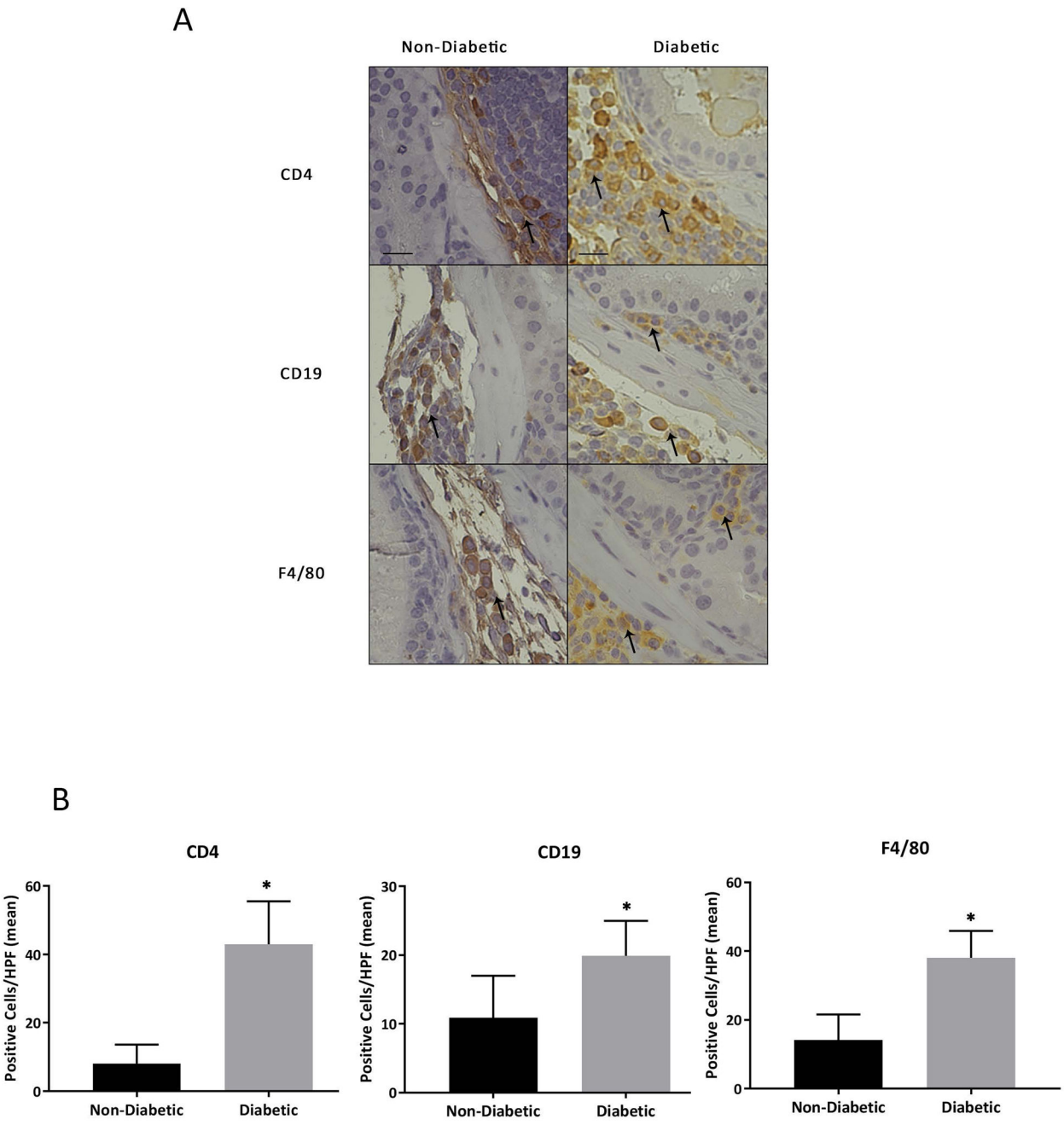

Figure 2. Increased Inflammatory Infiltrate is Associated with a More Severe Prostatic Phenotype

A) IHC staining of CD4+ T-cells, CD19+ B-cells, and F4/80+ macrophages. Staining reveals positive inflammatory cell marker expression in both non-diabetic and diabetic NOD mice.

B) Quantitation of inflammatory cell clusters shows a significant increase in overall inflammation in diabetic NOD mice.

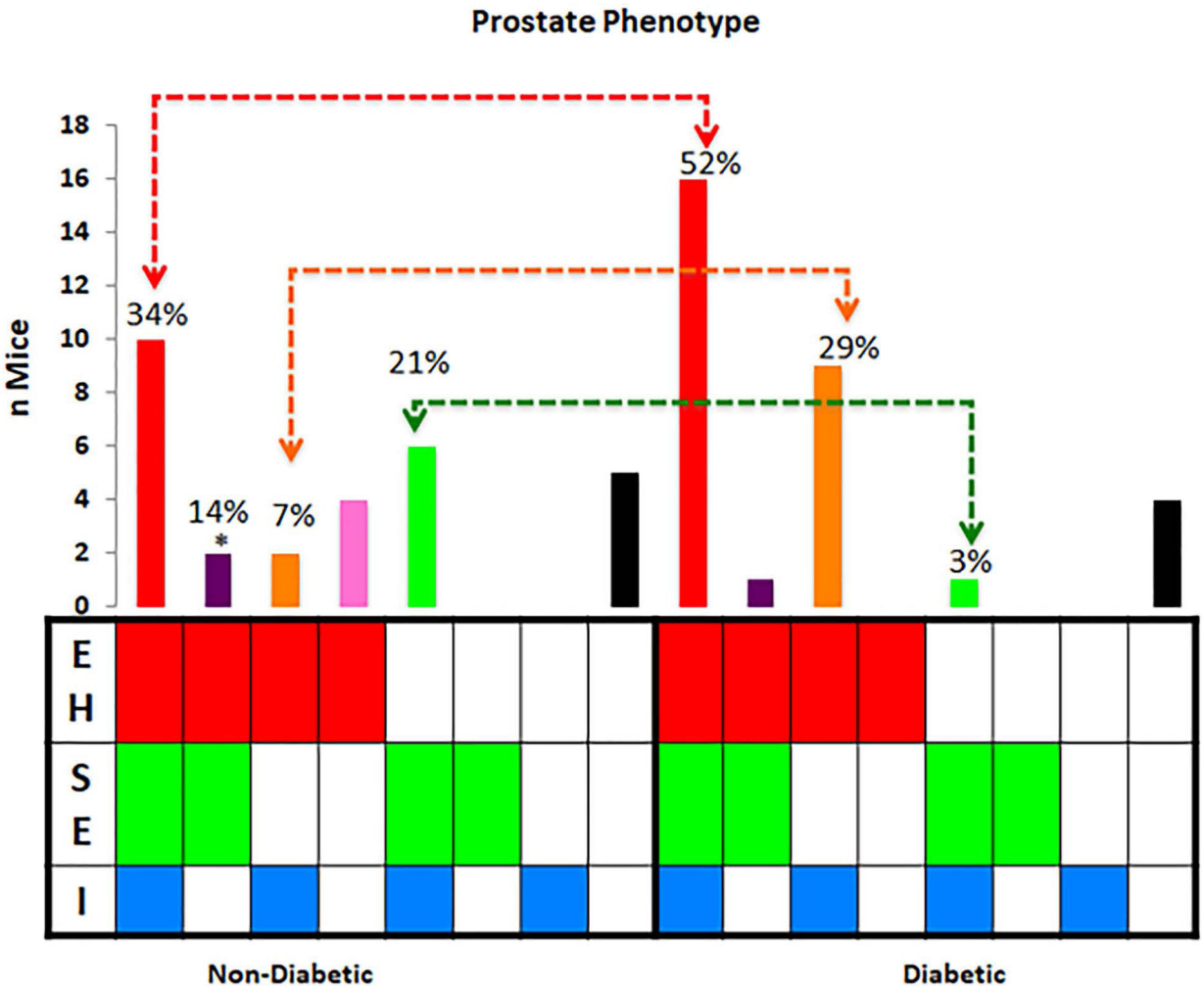

Figure 3. Association of Inflammation with Prostatic Phenotypes

Inflammatory infiltration (I) in the prostate is associated with epithelial hyperplasia (EH) + stromal expansion (SE) and EH only phenotypes in the non-diabetic while SE phenotype is more common in the diabetic NOD mouse *EH in the absence of SE and I is more common in the diabetic NOD mouse.

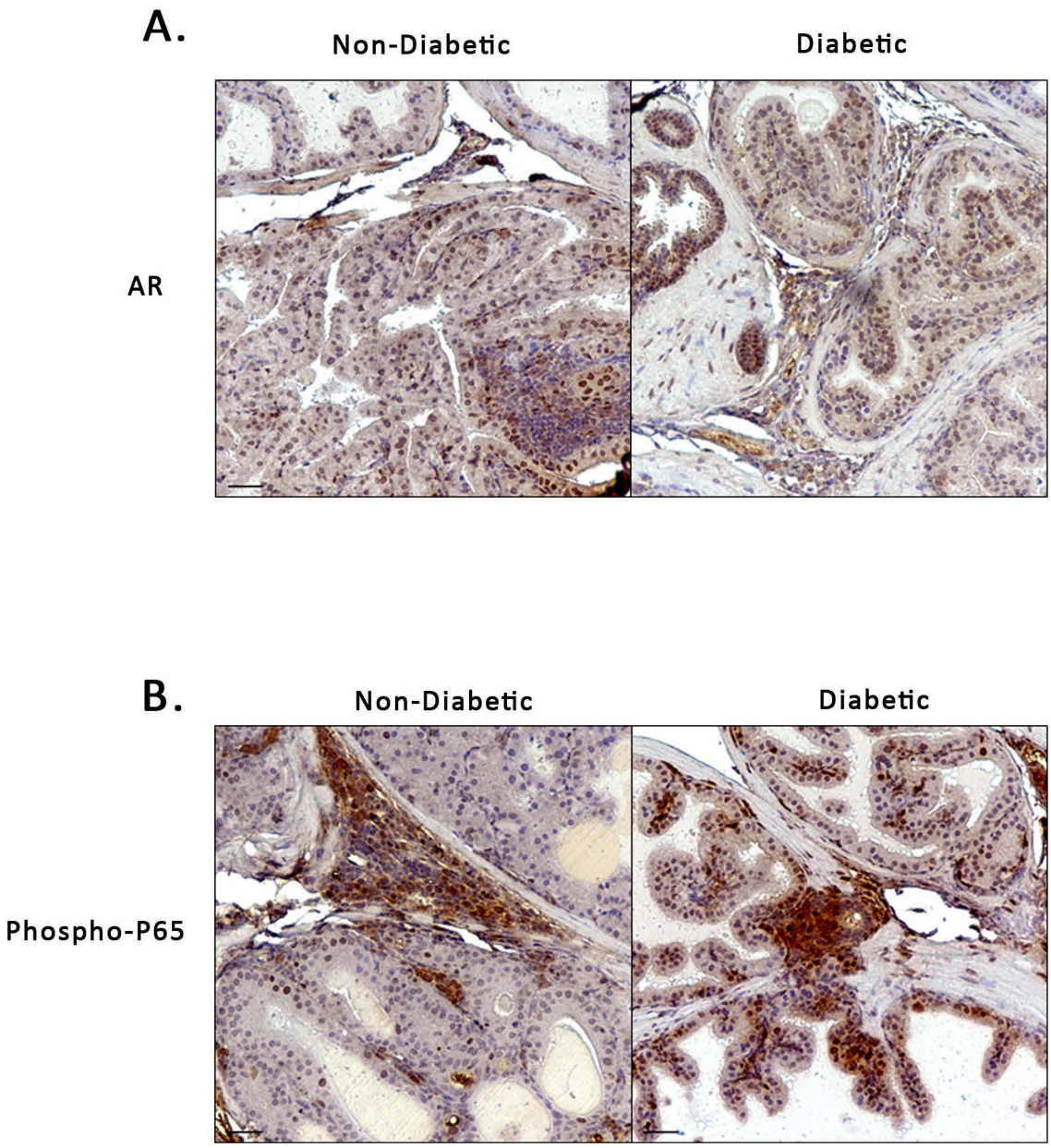

Figure 4. Androgen Receptor Expression and NF-κB activation in NOD Mouse Prostate

A) IHC staining showing positive Androgen Receptor (AR) expression in both non-diabetic and diabetic NOD mouse prostates. **B)** Positive IHC staining for NF-κB (Phospho-P65) in non-diabetic and diabetic NOD mouse, particularly in areas of and adjacent to inflammation.

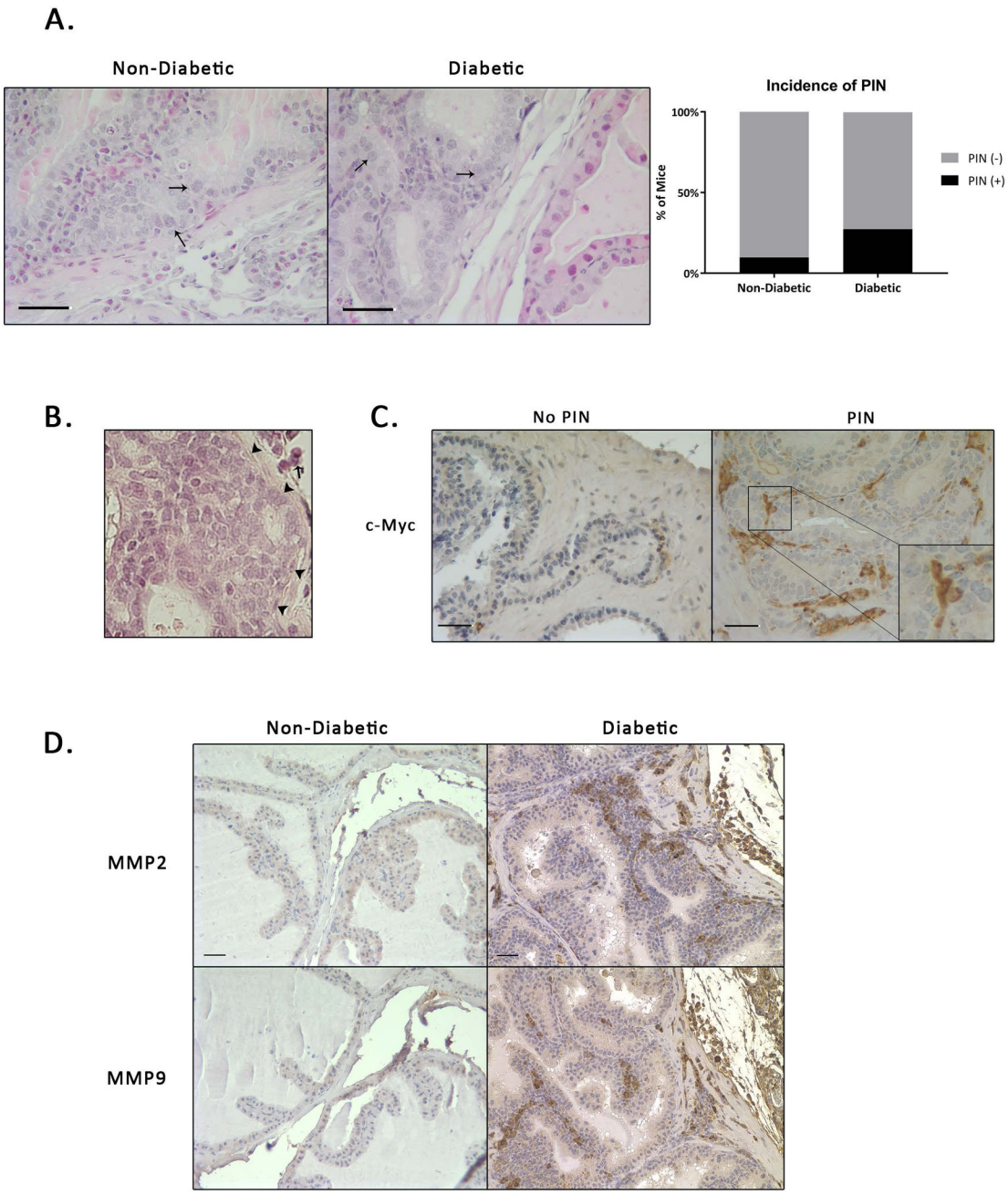

Figure 5. A Subset of Male NOD Mice Develop Areas of PIN-Like Changes

A) Areas of PIN-like changes in non-diabetic (ND) and diabetic (Di) mice. Arrows indicate enlarged nuclei or increased nuclear-cytoplasmic ratio. **B)** Representative H&E staining showing no breakdown of extracellular matrix in areas of PIN (arrowheads indicate intact basement membrane, arrow indicates inflammation) **C)** c-Myc staining revealed positive expression in regions with PIN-Like changes. **D)** MMP2 and MMP9 staining show increased expression in diabetic mice.

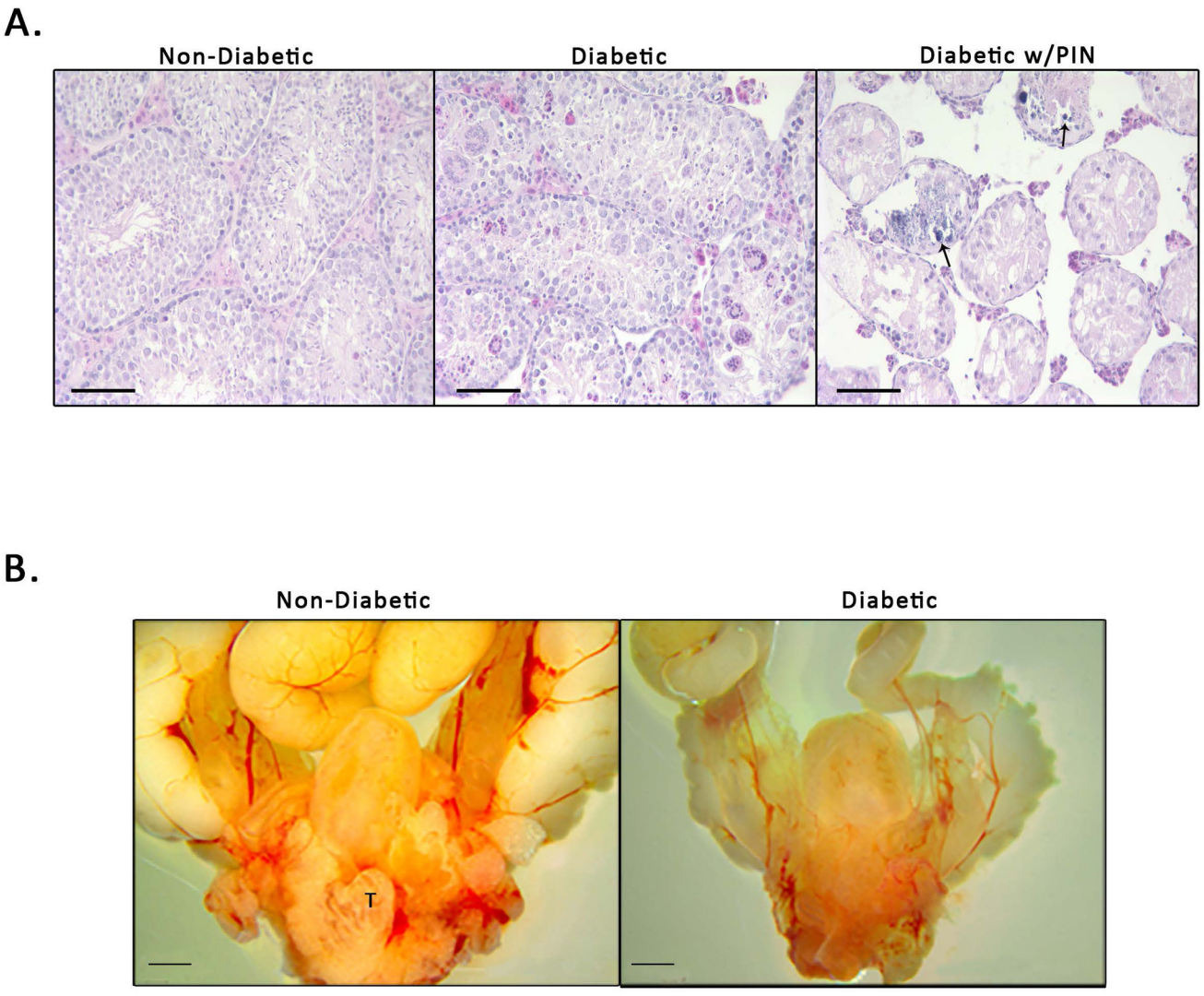

Figure 6. Diabetic Status is Associated with Testicular Changes in the NOD Mouse Prostate

A) Testicular phenotypes in non-diabetic mice (ND), diabetic mice (Di), and diabetic mice with PIN-like changes (Dp). ND mice appear to have normal phenotypic composition. Di mice exhibit calcification of the testes and cellular atrophy (arrows indicted areas of calcification). Dp mice have complete loss of testicular architecture, loss of Leydig cells, and severe cellular atrophy. **B)** Gross anatomy shows a decrease in the overall size of the urogenital tract in diabetic NOD mice compared to non-diabetic NOD mice (T indicates visible testis in non-diabetic mouse).

A

Comparison	Gene Symbol
Di vs. ND	Uts2b*
Dp vs. Di	Ang3
	Gzma
	Gzmb
	Krt19
	Ugt2b34

B

Comparison	Gene Symbol	Gene Symbol
Dp Vs. ND	Ang3	Igtp
	Ano9	Iigp1
	Casp12	Inmt
	CCL12	Irf7
	CCL3	Irgm2
	Cd7	Mark1
	Cd8a	Nkg7
	Cse1l	Pnliprp2
	Defb1	Rtp4
	Dsc1	Sectm1b
	Ebf4	Sh3bp2
	Echdc1	Slc39a4
	Ets2	Tgtp2
	Gm12185	Tnfsf10/TRAIL
	Gm12250	Ugt2b34
	Gzma	Vtcn1
	Gzmb	Zfp143

C

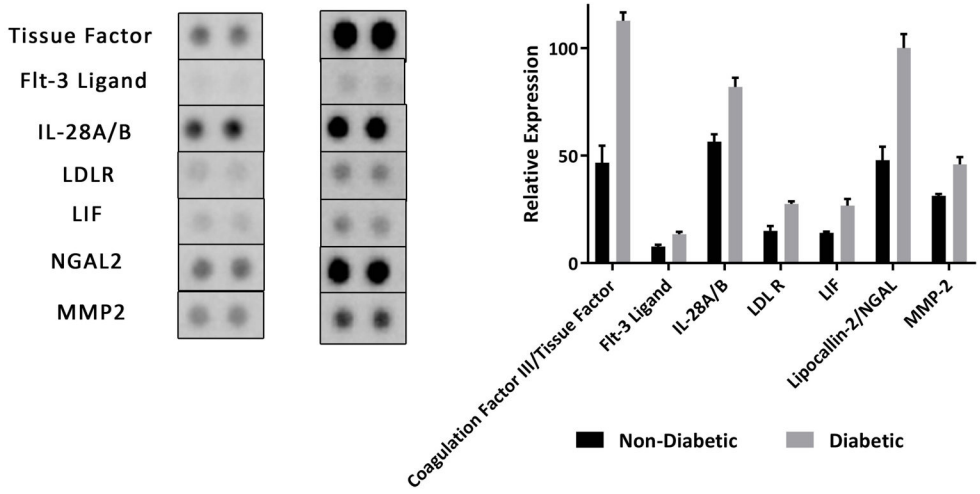

Figure 7. Differentially Expressed Genes and Cytokines in Male NOD Mice

A) Microarray analysis revealed 1 differentially expressed gene (DEG) in diabetic NOD mice vs non-diabetic NOD mice and 5 DEGs in diabetic NOD mice with PIN-like changes vs diabetic NOD mice. **B)** There were 34 DEGs in diabetic NOD mice with PIN-like changes vs non-diabetic NOD mice. Inflammatory related genes are highlighted in yellow. **C)** Results from cytokine array analysis reveal significant increase in seven analytes in diabetic NOD mice compared to non-diabetic NOD mice.

Table 1.

List of antibodies and reagents

Antibody/Reagent	Vendor	Stock Number	Dilution
CD4	Bio Rad Laboratories	MCA4635GA	1:200
F4/80	Bio Rad Laboratories	MCA497GA	1:100
CD19	Cell Signaling Technology	3574S	1:100
cMyc	Abcam	AB32072	1:250
Ki67	Abcam	AB16667	1:100
MMP2	Abcam	AB37150	1:4000
MMP9	Abcam	AB38898	1:100
NFkB pP65 (phospho)	Abcam	AB106129	1:100
BrdU	ThermoFisher Scientific	MA1-81890	1:200
VectaStain ABC Universal Elite Kit	Vector Laboratories	PK-6200	
Affymetrix Clariom S Assay, Mouse	ThermoFisher Scientific	902930	